ICSV13 - Vienna
The Thirteenth International Congress on Sound and Vibration
Vienna, Austria, July 2-6, 2006

AN INNOVATIVE HYBRID CFD/BEM METHOD FOR THE PREDICTION OF BODY-TURBULENCE INTERACTION NOISE

Christophe Schram and Michel Tournour

LMS International, Interleuvenlaan 68, Researchpark Haasrode Z1, 3001 Leuven, Belgium
christophe.schram@lms.be

Abstract

The increasing public awareness and concerns with respect to aerodynamically generated noise has led Computational Acoustics (CA) and Computational Fluid Dynamics (CFD) communities to develop the so-called hybrid approach, where the flow description obtained by CFD is used to synthesize equivalent aeroacoustic sources that are injected into a CA code. We propose an original implementation of the hybrid approach based on Curle's analogy, which formally describes the mechanism of sound generated by body-turbulence interaction. The originality stands in the separate handling of the effects of the body as source and scattering entity by the flow and acoustic solvers. The acoustic propagation is carried out using an acoustic code based on the Boundary Element Method (BEM), in which scattering by arbitrary geometries can be computed, including impedance effects where needed. Preliminary results are presented, validating the numerical handling of the pressure fluctuations as equivalent dipoles, and showing that the acoustical scattering is effectively accounted for by source surfaces, which was not the case with the conventional approach.

INTRODUCTION

The problem of sound generation by turbulence interacting with solid surfaces was given its first formal treatment through Curle's analogy [1]. This analogy considers the integral solution of Lighthill's analogy [2], written in differential form

$$\frac{\partial^2 \rho'}{\partial t^2} - c_0^2 \frac{\partial^2 \rho'}{\partial x_i^2} = \frac{\partial^2 T_{ij}}{\partial x_i \partial x_j} \qquad (1)$$

where $T_{ij} \equiv \rho v_i v_j + \left(p' - c_0^2 \rho'\right)\delta_{ij} + \sigma_{ij}$ is Lighthill's tensor, $\mathbf{v}$ is the fluid velocity, σ_{ij} is the viscous stress tensor, $\rho' \equiv \rho - \rho_0$ is the perturbation density chosen as acoustic variable, and $p' \equiv p - p_0$. The indexed quantities c_0, ρ_0 and p_0 are the

speed of sound, density and pressure in the quiescent and uniform medium taken as reference state in the propagation region. The density perturbation is caused by compressibility effects and non-isentropic effects. The pressure perturbation is related to momentum exchange, and also for isentropic flows to compressibility effects and density fluctuations through the definition of the speed of sound $c_0^2 \equiv \left(p'/\rho'\right)_{s=cst}$.
The integral solution of the differential equation (1) is classically obtained making use of a Green's function $G(t,\mathbf{x}|\tau,\mathbf{y})$, solution of the same inhomogeneous wave equation as (1), but where the right-hand-side is replaced by a Dirac pulse emitted at the position $\mathbf{y}$ and time τ:

$$\rho'(\mathbf{x},t) = \int_{-\infty}^{t}\int_{V} G\,\frac{\partial^2 T_{ij}}{\partial y_i \partial y_j}\,\mathrm{d}^3\mathbf{y}\,\mathrm{d}\tau - c_0^2\int_{-\infty}^{t}\int_{\partial V}\left(\rho'\frac{\partial G}{\partial y_i} - G\frac{\partial \rho'}{\partial y_i}\right)n_i\,\mathrm{d}^2\mathbf{y}\,\mathrm{d}\tau \qquad (2)$$

where V is the integration volume extending over the whole source region excluding the region occupied by the solid body, and ∂V is the boundary of this region, comprising the body surface. The first integral in (2) represents the noise produced by the double divergence of Lighghill's tensor in the bulk of the fluid contained in V, and the second integral represents the acoustic scattering of this incident sound over the boundaries. After a number of simplifications, discussed below, one obtains:

$$\rho'(\mathbf{x},t) = \int_{-\infty}^{t}\int_{V}\frac{\partial^2 G}{\partial y_i \partial y_j}\,T_{ij}\,\mathrm{d}^3\mathbf{y}\,\mathrm{d}\tau - \int_{-\infty}^{t}\int_{\partial V} p'\,\frac{\partial G}{\partial y_i}\,n_i\,\mathrm{d}^2\mathbf{y}\,\mathrm{d}\tau \qquad (3)$$

where the first term is equivalent to an acoustical quadrupole, and the second term represents an acoustical dipole. Adopting a free field Green's function, Curle showed in [1] that at low Mach numbers $M = U/c_0$ and low Helmholtz numbers $He = 2\pi\, f\, D/c_0$ – i.e. for a source acoustically compact, the ratio of the acoustic energies emitted by the quadrupolar and dipolar contributions scales as M^2. Neglecting the quadrupolar contribution is therefore justified at low-Mach numbers, which makes Curle's analogy quite powerful in applications such as noise produced by side mirrors, antennas, landing gears or wind turbine blades exposed to atmospheric turbulence, at least up to the low frequencies associated to large-scale turbulent structures. The solution (3) can be implemented following a so-called hybrid approach: the flow field is resolved in a first stage, and the sound field is determined in a second step, using Lighthill's tensor and the pressure fluctuations provided by the flow model in Eq. (3). This uncoupled way of processing of the flow data does naturally prescribe any acoustic feedback to the source flow region, where the density is usually assumed to be equal to the reference density ρ_0. Excluding situations where aero-acoustical resonance occurs, this approximation is usually quite reasonable at low Mach numbers. However, certain problems can arise that are related to the assumptions that were introduced to obtain Eq. (3). The first assumption, easily verified, considers the solid surface of the body to be steady, with a no-slip and no-penetration velocity boundary condition. The second hypothesis consists in neglecting the contribution of the viscous stresses to the net reaction force exerted by the body on the fluid. This hypothesis, discussed by Morfey [3], should be relevant in industrial applications where high-Reynolds flow separation dominates the force spectrum at the wall. The third assumption, which is seldom recognised as such in the literature, consists in considering that the flow model, used to provide Lighthill's equivalent source tensor, accounts for compressibility effects over the surface of the body located in the source region. This crucial assumption is involved in the derivation of Eq. (3), allowing to substitute the scattering integral in Eq. (2) by the dipole source integral [4]. The present paper addresses the pertinence of this assumption, and proposes an alternative implementation of Curle's analogy when it proves irrelevant, such as when an incompressible flow model is used to describe a non-compact equivalent source.

CURLE'S ANALOGY USING AN INCOMPRESSIBLE FLOW MODEL

The issue shows up when the dimensions of the solid body in the source region become comparable to, or exceed the wavelength of the sound it produces. Two examples of such situation can be evoked. The first one concerns the high-frequency component of the broadband noise produced by a turbulent boundary layer developing over an airfoil and being convected past its trailing edge, known as trailing-edge noise [6]. The second example concerns the sound produced by turbulence developing in ducts. In both cases, the region where turbulence interacts with the solid body extends over several acoustical wavelengths, and the acoustical scattering must be accounted for in the flow model. However, at low Mach numbers, incompressible flow simulations are often used to describe the source region. The density perturbations are in that case not contained within Lighthill's tensor, which is approximated by: $T_{ij} \approx T_{ij}^{inc} \equiv \rho_0 v_i v_j + p' \delta_{ij} + \sigma_{ij}$, where the pressure perturbation, when evaluated at the wall, is now exclusively associated to the incompressible conversion of wall-normal momentum into pressure across the boundary layer. The pressure perturbations in the surface integral of Eq. (3) are fairly uninfluenced by compressibility effects at low Mach numbers [5]. Indeed, for isentropic flows at low Mach numbers, the compressible, acoustic component of the pressure perturbation is quite small compared to the pressure perturbation resulting from the conversion of wall-normal momentum across the unsteady turbulent boundary layer. If the incompressible Lighthill tensor is used in Eq. (2), Eq. (3) becomes (neglecting the viscous stress contribution and with a no-slip boundary condition at the wall):

$$\begin{aligned} \rho'(\mathbf{x},t) = & \int_{-\infty}^{t} \int_{V} \frac{\partial^2 G}{\partial y_i \partial y_j} T_{ij} \, \mathrm{d}^3\mathbf{y} \, \mathrm{d}\tau - \int_{-\infty}^{t} \int_{\partial V} p' \frac{\partial G}{\partial y_i} n_i \, \mathrm{d}^2\mathbf{y} \, \mathrm{d}\tau \\ & - c_0^2 \int_{-\infty}^{t} \int_{\partial V} \left(\rho' \frac{\partial G}{\partial y_i} - G \frac{\partial \rho'}{\partial y_i} \right) n_i \, \mathrm{d}^2\mathbf{y} \, \mathrm{d}\tau \end{aligned} \qquad (4)$$

where the acoustic scattering is explicitly calculated over the surface of the body. One way to alleviate the difficulty of evaluating the scattering over the body surface consists in using a Green's function that is tailored to the body such that its normal derivative vanishes over the surface. This approach has been adopted for airfoil selfnoise prediction, by using either a half-plane Green's function or semi-analytical methods such as Schwarzchild's technique [6], or using approximated compact Green's functions for low-Mach numbers [7]. In extended duct systems however, there exists only a very limited number of idealized cases where analytical Green's functions can be obtained, and the scattering must be calculated numerically. The next section is devoted to the development of a specific implementation of Curle's analogy to be used with incompressible flow data where the source and scattering effects of the body are decoupled, the latter being computed by the Boundary Element Method of the commercial software SYSNOISE Rev5.6.

BOUNDARY ELEMENT FORMULATION OF CURLE'S ANALOGY

Boundary Integral Equations are usually written considering the acoustical pressure perturbation as unknown, and with the wave equation written in the frequency domain. Equation (1) is then written as a Helmholtz equation:

$$\nabla^2 \hat{p}_a + k^2 \hat{p}_a = \hat{q}_L \tag{5}$$

where $c_0^2\, \rho' = p'_a = \hat{p}_a\, \mathrm{e}^{i\omega t}$, $k = \omega / c_0$ and $\hat{q}_L = -\partial^2 \hat{T}_{ij} / \partial x_i \partial x_j$ with $T_{ij} \equiv \hat{T}_{ij}\, \mathrm{e}^{i\omega t}$. The Helmholtz equation (5) is resolved using the free field Green's function in frequency domain $G = \mathrm{e}^{-ikr} / 4\pi r$ (with $r = |\mathbf{x} - \mathbf{y}|$), solution of $\nabla^2 G + k^2 G = -\delta(\mathbf{x} - \mathbf{y})$. Combining Eq. (5) with the Helmholtz equation for the Green's function, we obtain:

$$\int_{V \setminus V_\varepsilon} \left(\nabla^2 p_a\, G - p_a\, \nabla^2 G \right)\ \mathrm{d}^3\mathbf{y} = \int_{V \setminus V_\varepsilon} q_L\, G\ \ \mathrm{d}^3\mathbf{y} + \int_{V \setminus V_\varepsilon} p_a\, \delta(\mathbf{x} - \mathbf{y})\ \ \mathrm{d}^3\mathbf{y} \tag{6}$$

where the volume V_ε has been subtracted from the volume V (see Figure 1) because the acoustic field is to be evaluated over the surface of the body itself, and the singularity of the Green's function kernel at $\mathbf{y} = \mathbf{x}$ must be excluded to perform the integrations by parts that follow. The point $\mathbf{y} = \mathbf{x}$ being not contained in $V \setminus V_\varepsilon$, the second integral of (6) is identically zero. Integrating by parts the LHS of (6) yields:

$$\begin{aligned} \int_{V \setminus V_\varepsilon} \left(\nabla^2 p_a\, G - p_a\, \nabla^2 G \right)\ \mathrm{d}^3\mathbf{y} &= \int_{\partial (V \setminus V_\varepsilon)} \left(\frac{\partial p_a}{\partial n} G - p_a \frac{\partial G}{\partial n} \right)\ \mathrm{d}^2\mathbf{y} \\ &= \int_{\partial V} \left(\frac{\partial p_a}{\partial n} G - p_a \frac{\partial G}{\partial n} \right)\ \mathrm{d}^2\mathbf{y} + \int_{\partial V_\varepsilon} \left(\frac{\partial p_a}{\partial n} G - p_a \frac{\partial G}{\partial n} \right)\ \mathrm{d}^2\mathbf{y}\,. \end{aligned} \tag{7}$$

The contribution of the last integral is evaluated for the limit of the exclusion volume (supposed spherical) dimension tending towards zero [8]:

$$\begin{aligned} &\lim_{\varepsilon \to 0} \int_{\partial V_\varepsilon} \left(\frac{\partial p_a}{\partial n} G - p_a \frac{\partial G}{\partial n} \right)\ \mathrm{d}^2\mathbf{y} \\ &= \lim_{\varepsilon \to 0} \int_0^{2\pi} \int_0^{\pi} \left(-\frac{\partial p_a}{\partial r} G + p_a \frac{\partial G}{\partial r} \right)_{r=\varepsilon} \varepsilon^2 \sin\theta\ \ \mathrm{d}\theta\, \mathrm{d}\varphi = -C(\mathbf{x})\, p_a(\mathbf{x}) \end{aligned} \tag{8}$$

where the factor $C(\mathbf{x})$ is the normalized solid angle seen by the point $\mathbf{x}$ in its exclusion volume V_ε, different from 1 when the point $\mathbf{x}$ lies on the surface of the acoustic mesh.

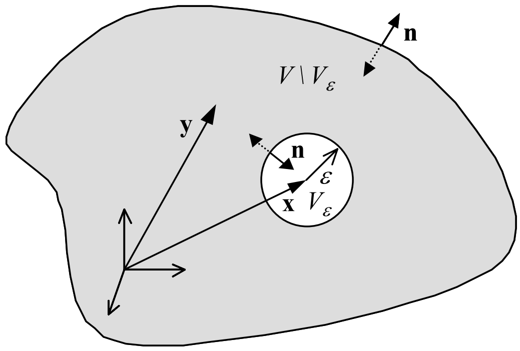

Figure 1: integration volume, excluding the Green kernel singularity at $\mathbf{x}=\mathbf{y}$.
The surface normal points outwards from the integration volume
(reversed in BEM convention: the dotted normal vector points outwards from the solid body).

Back-substituting (7) and (8) into Equation (6) gives:

$$C(\mathbf{x})\,p_a(\mathbf{x}) = \int_{\partial V} \left(\frac{\partial p_a}{\partial n} G - p_a \frac{\partial G}{\partial n} \right) \mathrm{d}^2\mathbf{y} + \lim_{\varepsilon \to 0} \int_{V \setminus V_\varepsilon} \frac{\partial^2 T_{ij}}{\partial y_i \partial y_j} G \;\; \mathrm{d}^3\mathbf{y} \qquad (9)$$

Performing the same treatment for the remaining volume integral, we find:

$$\begin{aligned} C(\mathbf{x})\,p_a(\mathbf{x}) = \int_V T_{ij} \frac{\partial^2 G}{\partial y_i \partial y_j} \;\mathrm{d}^3\mathbf{y} + \int_{\partial V} \left(-c_0^2 \frac{\partial \rho_L}{\partial n} G - \left(p_L - c_0^2\,\rho_L\right) \frac{\partial G}{\partial n} \right) \mathrm{d}^2\mathbf{y} \\ - C(\mathbf{x})\left(p_L(\mathbf{x}) - c_0^2\,\rho_L(\mathbf{x})\right) + \int_{\partial V} \left(\frac{\partial p_a}{\partial n} G - p_a \frac{\partial G}{\partial n} \right) \mathrm{d}^2\mathbf{y} \end{aligned} \qquad (10)$$

where the sub-index L has been introduced to indicate quantities that derive from Lighthill's tensor, provided by a suitable flow model.

Introducing the decomposition $p_L \equiv p_a + p_h$, where p_a is associated to an isentropic compression and p_h is the hydrodynamic component, Eq. (10) can be interpreted in two ways:

1. The source description satisfies the isentropic, compressible flow equations. In that case, Equation (10) becomes:

$$C(\mathbf{x})\,p_L(\mathbf{x}) = \int_V T_{ij} \frac{\partial^2 G}{\partial y_i \partial y_j} \;\mathrm{d}^3\mathbf{y} - \int_{\partial V} p_L \frac{\partial G}{\partial n} \;\mathrm{d}^2\mathbf{y} \qquad (11)$$

which is analogous to the classical Curle analogy: the surfaces wetted by turbulence act as pure sources, acoustic scattering is not to be evaluated over these surfaces. A subtle difference is however that Eq. (11) provides directly the total (hydrodynamic and compressible) pressure field, as a result of placing the listener in the flow field. The usual acoustic pressure perturbation is obtained by placing the listener in the quiescent and uniform medium that is generally considered in the propagation region.

2. The source description is obtained by an incompressible flow model. The density fluctuations are not captured by the flow solution, and Eq. (10) becomes, assuming a steady surface where $\partial p_a / \partial n = 0$:

$$C(\mathbf{x})\, p_a(\mathbf{x}) = \int_V T_{ij} \frac{\partial^2 G}{\partial y_i \partial y_j}\ \mathrm{d}^3\mathbf{y} - \int_{\partial V} (p_a + p_h) \frac{\partial G}{\partial n}\ \mathrm{d}^2\mathbf{y} - C(\mathbf{x})\, p_h(\mathbf{x}) \qquad (12)$$

Remarkably, both formulations (11) and (12) appear as formally identical using the decomposition $p_L = p_a + p_h$. The difference is that in Eq. (11), the total pressure p_L is given as input from the flow description, and resolved over the body surface; while in Eq. (12), the hydrodynamic component p_h is given and the acoustic component p_a is resolved. A Boundary Element discretisation of the boundary integrals is implemented for the resolution of the acoustic pressure.

The BEM approach consists in decomposing the continuous surface into small surface elements, where the continuous unknown field is approximated by a nodal expansion: $p(\mathbf{y}) = \sum_{i=1}^{n_e} N_i^e(\mathbf{y})\, p_i$ where p_i is the value taken by the pressure field at the node i of the element e. In matrix form, this yields at the collocation node k:

$$C_k\,(p_{ak} + p_{hk}) = [A'_{ki}]\,(\{p_{ai}\} + \{p_{hi}\}) + q_k \quad \text{or} \quad [A_{ki}]\{p_{ai}\} = -[A_{ki}]\{p_{hi}\} + q_k \qquad (13)$$

where

$$[A'_{ki}] = \sum_{i=1}^{N_i} \left(\sum_{e=1}^{n_i} \int_{\partial V_e} N_i^e(\mathbf{y}) \frac{\partial G(\mathbf{x}_k, \mathbf{y})}{\partial n}\ \mathrm{d}^2\mathbf{y} \right), \qquad [A_{ki}] = C_k\,[\delta_{ki}] - [A'_{ki}] \qquad (14)$$

and q_k is the incident field emitted by the volumetric source of Equation (12).

PRELIMINARY RESULTS

The first validation case concerns an external propagation problem, in which periodic forces applied to a sphere radiate in free field. In the present case, the frequency considered makes the sphere compact, such that the classical form of Curle's analogy is implemented. The purpose is to validate quantitatively the amplitude of the sound field calculated from the BEM discretisation. Pressure fluctuations are spatially generated over the surface of the sphere with unit radius (2400 elements), following a cosine of the polar angle (see Figure 2). The sound pressure is obtained at a field point located on the z-axis, at a distance equal to 1000 sphere radii. The frequency is 1 Hz, making the sphere effectively compact (1/340$^{\text{th}}$ of the wavelength). The differences of retarded time can therefore be neglected. The pressure is in far field $p(r,\theta,\omega) = i\omega F \cos\theta / (4\pi c_0 r)\, \mathrm{e}^{-ikr}$ where the net force $F = 4\pi/3\,\mathrm{N}$, placed at the centre of the sphere, is obtained by surface integration of the hydrodynamic pressure.

We obtain a theoretical acoustical pressure amplitude equal to 6.16×10^{-6} Pa at the field point. The calculation yields an acoustical pressure amplitude of 6.15×10^{-6} Pa. The same correct result was obtained using the 'incompressible dipole' formulation (12).

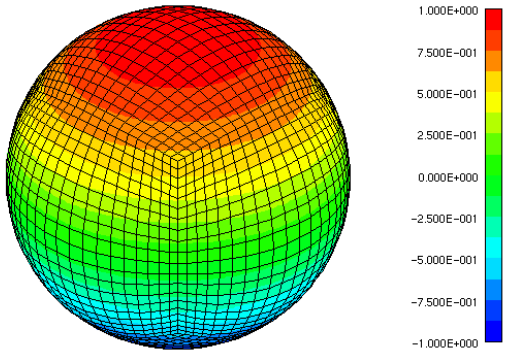

Figure 2: sphere with cosine dipole distribution.

The second validation case concerns an internal acoustic propagation problem. Dipoles with unit amplitude have been applied over a frequency range from 10 to 50 Hz with 0.1 Hz interval, over one face at the extremity of a 10 meters long duct, with a 1 m x 1 m square section. The problem is first solved using the 'compressible dipole' formulation (11) (with no volumetric source term), therefore assuming that the pressure data accounts for compressibility effects, and in particular for the acoustic scattering. The 'incompressible dipole' formulation (12) has been applied in a second step. The pressure is evaluated in both cases at a field point located at 2 m from the duct end opposite to the dipole B.C. face, on the duct centreline. The first two acoustical resonances, correspond to longitudinal modes at frequencies of 17 Hz and 34 Hz, are seen in Figure 3 to be correctly captured using the 'incompressible dipole' formulation, while the 'compressible dipole' formulation yields results with no apparent resonance.

The difference is due to the fact that according to the classical Curle analogy, the scattering is simply not computed over the parts of the boundary mesh where dipoles are generated from the flow data, on the assumption that the dipoles account themselves for the scattering. At the opposite, the source and scattering effects are decoupled in the formulation (13), so that the flow description should not capture acoustical effects, which are handled by the BEM solver. The situation is more ambiguous in cases where low-order compressible CFD simulation is used to model the source, such methods being known to capture localized acoustic propagation, but dissipate this information within a certain fraction or couple of wavelengths away from the source. Ad-hoc coupling schemes must be devised to account for the variety of cases depending on the effective compressibility achieved by the flow model. This is the subject of future developments.

CONCLUSIONS AND PERSPECTIVES

Curle's aeroacoustical analogy has proved its usefulness in applications where the acoustical scattering is accounted for by the flow model, or when scattering can be neglected owing to acoustical compactness. A straightforward application of the classical form of this analogy is however inadequate when the extend of the sound-generating body extends over several acoustical wavelengths and when the flow data accounts imperfectly for acoustical effects over its surface, such as when incompressible or low-order compressible CFD is used to model the flow in the source region. An alternative form of Curle's analogy has been developed and implemented in a Boundary Element Method, which decouples the roles of the body surface as a source and scattering entity. The method has been validated quantitatively and qualitatively, in the case of a compact source in free field and for an internal propagation problem, using arbitrary pressure fluctuations to model the source. Further validations are planned, which include realistic configurations where the flow data is provided through incompressible and low-order compressible Computational Fluid Dynamics simulations.

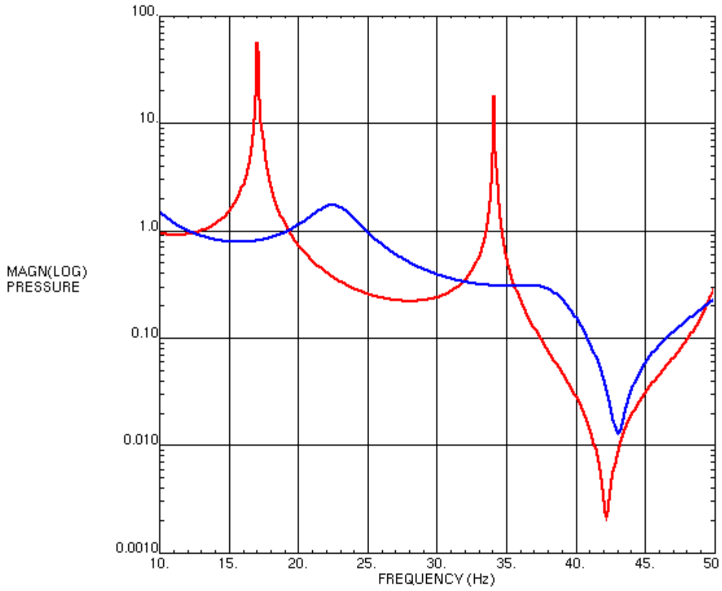

Figure 3: duct resonances obtained with the incompressible dipole formulation (red curve), and absent using the compressible dipole formulation (blue curve).

References

[1] N. Curle, "The influence of solid boundaries upon aerodynamic sound", Proc. Roy. Soc. Lond., **A23**, 505-514 (1955).

[2] M.J. Lighthill, "On sound generated aerodynamically, Part 1: general theory", Proc. Roy. Soc., **A211**,564-587 (1952).

[3] C.L. Morfey, "The role of viscosity in aerodynamic sound generation", Int. J. Aeroacoustics, **2**, 225-240 (2003).

[4] C. Schram, J. Anthoine, A. Hirschberg, "Calculation of sound scattering using Curle's analogy for non-compact bodies", 11th AIAA/CEAS Aeroacoustics Conference, Monterey, Paper 2005-2836 (2005).

[5] M. Wang, J.B. Freund, S.K. Lele, "Computational prediction of flow-generated sound", Ann. Rev. Fluid Mech., **38**, 483-512, (2006).

[6] M. Roger, S. Moreau, "Back-scattering correction and further extensions of Amiet's trailing edge noise model. Part I: theory", J. Sound Vib., **286**,477-506 (2005).

[7] M. Howe, *Theory of Vortex Sound* (Cambridge texts in applied mathematics, Cambridge, 2003).

[8] O. von Estorff, *Boundary Elements in Acoustics, Advances and Applications* (WIT Press, 2000).